Desalination and Water Treatment
www.deswater.com
doi: 10.5004/dwt.2021.27883

243 (2021) 123–142
December

Antifouling enhancement of polyethersulfone membranes incorporated with silver nanoparticles for bovine serum albumin and humic acid removal

Maryam Al-Bulushi[a,b], Muna Al-Hinai[c], Sulaiman Al-Obaidani[d], Sergey Dobrestov[e,f], Edward Nxumalo[g], Mohammed Al-Abri[a,b,*]

[a]*Department of Petroleum and Chemical Engineering, College of Engineering, Sultan Qaboos University, P.O. Box: 33, PC 123, SQU, A-Khoudh, Oman, emails: alabri@squ.edu.om (M. Al-Abri), eng.maryam.al-bulushi@hotmail.com (M. Al-Bulushi)*
[b]*Nanotechnology Research Centre, Sultan Qaboos University, P.O. Box: 17, PC 123, SQU, Al-Khoudh, Oman*
[c]*Department of Process Engineering, International Maritime College Oman, P.O. Box: 532, PC 322, Falaj Al Qabail, Sohar, Oman, email: muna.alhinai@imco.edu.om*
[d]*Department of Mechanical and Industrial Engineering, College of Engineering, Sultan Qaboos University, P.O. Box: 33, PC 123, SQU, A-Khoudh, Oman, email: sobeidani@squ.edu.om*
[e]*Department of Marine Science and Fisheries, College of Agricultural & Marine Sciences, Sultan Qaboos University, P.O. Box: 34, Al-Khoudh, Muscat 123, Oman, email: sergey@squ.edu.om*
[f]*Center of Excellence in Marine Biotechnology, Sultan Qaboos University, P.O. Box: 50, Al-Khoudh, Muscat 123, Oman*
[g]*Institute for Nanotechnology and Water Sustainability, College of Science, Engineering and Technology, University of South Africa, Roodepoort 1709, South Africa, email: nxumaen@unisa.ac.za*

Received 12 June 2021; Accepted 13 October 2021

ABSTRACT

Enhanced antifouling polyethersulfone (PES) ultrafiltration membranes were successfully modified by the incorporation of silver nanoparticles (AgNPs) for improved disinfection in water treatment applications. PES-AgNPs membranes were fabricated with AgNPs loading (0.0–2.0 wt.%) via the phase inversion method. The effect of AgNPs on PES physicochemical properties and membrane performance were investigated in terms of pure water flux, filtration of humic acid (HA) and bovine serum albumin (BSA), and antibacterial activity. The antifouling property of the membrane was analyzed by calculation of the fouling resistance parameters of BSA. The antibacterial activity of the membrane was tested using two different types of bacteria which are *Bacillus subtilis (B. subtilis)* and *Escherichia coli (E. coli)*. Hydrophilicity/hydrophobicity evaluation of the membranes was studied by water contact angle measurement which was reduced from 68° for the pristine PES membrane to 58° for the PES-0.5AgNPs membrane. The PES-0.5AgNPs membrane displayed improved water flux by 65.55% and both HA and BSA rejections were 90.04% and 82.41%, respectively. Although the surface hydrophilicity of the PES-AgNPs membrane was further decreased at higher silver loading (1.0 and 2.0 wt.%), the mechanical properties of nanocomposite membranes were reduced and significant silver leaching was observed. A high BSA flux recovery of about 97.29% was achieved for the modified membrane with 2.0 wt.% AgNPs compared to 71.12% for the neat membrane. In terms of the antibacterial performance, PES-AgNPs membranes showed an excellent property in biofouling mitigation where *E. coli* results show more sensitivity to AgNPs than *B. subtilis*. Based on the findings, the PES-AgNPs nanocomposite membrane offers a good potential membrane for filtration and disinfection.

Keywords: Polyethersulfone; Silver nanoparticles; Humic acid; Bovine serum albumin; Antibacterial; Water treatment

* Corresponding author.

1. Introduction

The unavailability and inaccessibility to clean water have become a global issue of concern as the human population grows and industrial and agricultural activities expand. Pure drinking water would be a major problem for developing countries in the world [1,2]. Freshwater is now extensively consumed around the world and people tend to reuse the freshwater from wastewater to protect the environment [3,4]. Desalination is the main technology for producing freshwater from brackish, seawater and other saline water sources. It depends on a pretreatment system to generate high-quality feed water to ensure stable and reliable operation of the reverse osmosis (RO) system. Pretreatment is the treatment of wastewater by industrial and commercial facilities to remove impurities from feed water before being fed to another system [3]. Current pretreatment methods such as flocculation and adsorption are based on a combination of physical, chemical, and biological processes and have succeeded to some extent in treating effluents for discharge purposes. Indeed, those methods cannot give a guarantee in terms of separation efficiency and effluent quality. In addition, these methods are often costly and ineffective [4].

Membrane technology is an essential part of water treatment facilities. It is a useful tool in separation, purification and fractionation processes emerging as a highly efficient technique over conventional methods [5]. This technology contributes up to 53% of the total world processes for the production of clean water [6]. Microfiltration (MF), ultrafiltration (UF), nanofiltration (NF) and RO membranes are some of the membrane types used for water treatment [7,8]. Among all, the UF system provides a positive barrier to remove most of the contaminants present in water and prevent damaging the RO membranes due to its unique advantages such as excellent separation efficiency, easy operation, low energy and maintenance costs, and little or no use of chemicals [9]. The selection of a technique for polymeric membrane fabrication depends on the choice of polymer and the desired structure of the membrane. The most commonly used techniques for the preparation of polymeric membranes include phase inversion, interfacial polymerization, stretching, track-etching and electrospinning [6,7,10]. The phase inversion technique is one of the main techniques for the fabrication of asymmetric porous structural UF membranes due to its simple processing, flexible production scales and low cost [7,10]. It is based on the principal transformation of homogenous polymer solution into a solid-state membrane [10].

Typical polymers used for UF membrane applications include polyacrylonitrile (PAN), polyvinylidene fluoride (PVDF), polysulfone (PS) and polyethersulfone (PES). Among all, PES has attracted a lot of attention as a polymer membrane because of its excellent properties such as thermal stability, good chemical properties, mechanical strength and low cost [11]. However, the hydrophobic nature of PES leads to membranes with high fouling propensity and consequently, the application of PES membranes in water treatment applications has been limited [11–13]. Chlorination is the most commonly used disinfection process to reduce biofouling. Nevertheless, it has several disadvantages, such as the formation of harmful disinfection by-products (DBP) and being ineffective to eliminate some types of microbes [2]. Thus, there is a strong need for membrane modification techniques to enhance membrane properties, prevent the biofouling problem and elongate the membrane lifetime [14]. Several methods have been proposed to enhance anti-fouling properties of PES membranes which can be classified into three categories including blending with other polymers, surface modification and incorporation of inorganic nanoparticles [14].

Generally, metal and metal oxide nanoparticles such as AgNPs [15–17], ZnO [18], FeO [19] and TiO_2 [20] have been utilized for the modification of polymeric membranes. Most of the work presented in the literature highlighted silver nanoparticles (AgNPs) as a good candidate in membrane fabrication due to the outstanding optical, high conductivity and antibacterial properties compared to the other nanoparticles [15–17]. It is agreed by many researchers that AgNPs are considered to be a promising antibacterial agent and can be applied in antimicrobial applications, water disinfection, pharmaceutics, composite fibers, cosmetic products, and electronic components [21]. Many methods exist to synthesize silver nanoparticles, Basri et al. [16] prepared an asymmetric PES membrane and studied the influence of additives ($AgNO_3$ and PVP of various M_w) on the structure of the prepared composite membrane. The performance of the membranes in the filtration and antibacterial test was evaluated with respect to the additives. It is observed in the study that, the PES-Ag membrane with 2.0 wt.% of Ag displayed high Ag-intensity, thus resulting in high antibacterial activity against *E. coli*. It was also commonly reported in the literature that the impregnation of silver into the membrane matrix could affect its morphology as well as membrane performance. An *ex-situ* method was reported by Rehan et al. [15] in which synthesis of AgNPs was carried out using chemical reduction of silver nitrate ($AgNO_3$) with fructose and using PVP as a capping agent. All membranes were prepared via a non-solvent induced phase separation (NIPS) process using PES as polymer. The amount of the AgNPs loading was selected from 0.0 to 0.64 wt.%. In this way, AgNPs were dispersed homogeneously in the polymer matrix and the addition of particles tended to suppress the formation of macro-voids. This can be attributed to the increase in viscosity of the solution and subsequently the decrease of the solvent/non-solvent exchange. In other work, Sile-Yuksel et al. [22] studied the effect of AgNPs location in polymer types. Three different polymers (PES, PS and CA) were used to fabricate nanocomposite membranes at three AgNPs different ratios (0.03, 0.06 and 0.09 w/w). The authors reported that AgNPs are homogeneously located along with the membrane matrix both in the skin layer and sublayer, but they protruded from the top surfaces of membranes. However, the increase of the AgNPs/polymer ratio tended to increase the water permeability of membranes.

On the other hand, numerous studies are claiming that incorporating AgNPs into the membrane matrix could promote antibacterial properties. This is due to the interaction of silver with sulfur-containing groups especially thiol groups of bacterial DNA [6]. Silver NPs provide a toxic effect upon its contact with the bacteria cell membrane, for which silver ions bind to the sulfur group and destabilized the protein of bacteria cells [6,11]. The antibacterial activity assay approaches are generally divided into qualitative

detection (growth inhibition zone for bacteria [17]) and quantitative measurement (plate-counting method [23]). The effect of $AgNO_3$ content on the antibacterial properties was reported by Chen et al., (2013). In that study, the PES membranes showed good antibacterial activity against *E. coli* after adding the $AgNO_3$ and the antibacterial rate of PES/$AgNO_3$ UF membrane with $AgNO_3$ content of 1.0 wt.% could reach 99.9% after running for 48 h [23]. In short, several positive attributes shown by AgNPs make it an excellent candidate to incorporate in PES membranes for water treatment.

The current study aims to improve the desirable characteristics for PES membranes (high water flux, solute rejection, and antifouling properties) while also improving their tensile strength and antibacterial properties using AgNPs as nano-additives. Based on a thorough survey of the literature, studies related to humic acid (HA) and bovine serum albumin (BSA) removal using PES ultrafiltration membrane impregnated with AgNPs for water treatment applications are rarely reported. Hence, there is the absence of understanding of the effect of AgNPs on PES physicochemical properties and membrane performance. To achieve this, PES membranes were prepared with and without AgNPs via a non-solvent induced phase separation method. Besides, samples were characterized using diverse analytical measurements including field emission scanning electron microscopy (FE-SEM), energy-dispersive X-ray spectroscopy (EDS), Fourier-transform infrared (FTIR) spectroscopy, X-ray diffraction (XRD), water contact angle (WCA), porosity and mechanical properties measurement techniques. The performance of the prepared membranes was investigated by pure water flux, HA and BSA rejection and fouling resistance of BSA. Finally, antibacterial activities of the membranes were carried out against *B. subtilis* as the model Gram-positive bacteria and *E. coli* as the model Gram-negative bacteria.

2. Experimental methods

2.1. Materials

Polyethersulfone (PES) pellets (molecular weight of 58,000 g mol^{-1} and density of 1.37 g cm^{-3}) were purchased from Goodfellow Cambridge Limited (England) and used as a basic polymer for membrane preparation. High purity 1-methyl-2-pyrrolidinone (NMP > 99%) was obtained from Fluka Analytical (Germany) and used as a solvent to dissolve the polymer. Inorganic hydrophilic silver nanoparticles (Ag, 99.99%, 30–50 nm, w/~0.2 wt.% PVP coated) were supplied by US Research Nanomaterials, Inc. HA and BSA (fraction powder 96%, M_w = 66.5 kDa) were used as model foulant for membrane solute rejection studies and supplied by Fisher Scientific. Sodium hydroxide (NaOH) (M_w = 40 g mol^{-1}, EMSURE, Germany) and sulfuric acid (H_2SO_4) (AnalaR, Germany) were added during HA preparation to improve humic acid solubility in water and to adjust the solution pH. *B. subtilis* (SQUMSF005) and *E. coli* (ATCC 25922) were prepared to evaluate the membrane biofouling performance. Acetone (AC > 99.5%) and deionized water were used for cleaning the tools that were used in membrane fabrication. Also, deionized water was used as the main non-solvent in the coagulation bath for preparing the membranes. All chemicals were utilized as received without further purification.

2.2. Fabrication of PES-AgNPs flat sheet membranes

Four PES-AgNPs ultrafiltration membranes were fabricated at a different weight percentage of AgNPs (0.0, 0.5, 1.0, 2.0 wt.%) loading into the membranes by *in situ* blending method. The phase inversion by the immersion precipitation technique was selected to fabricate polymeric membranes [15,24]. Prior to the preparation of the casting solution, PES pellets (15 wt.%) were dried in an oven at 70°C overnight to remove moisture which could influence the performance of the membrane during the fabrication process. The membrane dope solutions were prepared through the following steps. First, adding a specific weight percent of AgNPs (30–50 nm) in the NMP solvent (82 mL) under constant stirring at 600 rpm. AgNPs were dispersed in NMP solvent with the assistance of sonication at 40 kHz for 45 min. Subsequently, dried PES pellets were added into the casting solution slowly under continuous stirring until the pellets completely dissolved to obtain homogenous solutions. The mixture was sonicated for another 40 min at ambient temperature to remove invisible air bubbles within the polymer solution. Before casting the membranes, the homogenous solutions were left for another hour to allow any bubbles to escape out the solution. Finally, the prepared dope solution viscosity was measured by using a rotational viscometer (Anton Paar, Austria).

After preparing a homogenous solution, the polymer solution was poured onto a glass plate that was used as a support for the casting film solution. The membrane casting thickness was maintained at 240 μm for all membranes [24]. Then, the glass plate with the thin-film of composite membranes was immersed immediately into a water bath at ambient temperature (~23°C ± 2°C) overnight. This process promoted phase inversion between the NMP solvent and the deionized water and thus activated the polymerization process [25]. During the process, a white membrane was obtained which was kept immersed in the aqueous bath for a day to ensure that all of the residues solvents in the membrane was removed. Then, the washed membranes were dried at ambient temperature followed by drying in the vacuum oven (20°C) for another day. Finally, the membrane was stored in the desiccator until further investigations.

2.3. Characterization of fabricated membranes

The surface morphology and cross-sectional images of PES and PES-AgNPs membranes were observed using a field-emission scanning electron microscope (FE-SEM, JEOL JSM-7600F, Japan) operated at a voltage of 20 kV and 8 mA. To avoid damage to the cross-section of membranes microstructure, all samples were freeze-fractured in liquid nitrogen and coated with gold by sputtering to obtain clear FE-SEM images. EDS equipped with FE-SEM was used to analyze elemental composition and dispersion of AgNPs within the fabricated membranes.

The chemical structure pattern and functional groups of the membrane surface were detected using attenuated total reflectance-Fourier-transform infrared spectroscopy

(ATR-FTIR) (PerkinElmer, USA) in the 4,000–400 cm^{-1} range with a signal wavenumber resolution of 4 cm^{-1} and an average of 32 scans.

The presence of AgNPs within membrane matrix was further confirmed by an XRD measurement using MiniFlex 600 (Rigaku, Japan) with a scanning rate of 2°/min and step extent of 0.01° equipped with a Cu-K_α radiation (wavelength (λ) = 1.5406 Å) at a tube voltage of 40 kV and a current of 15 mA.

For hydrophilicity/hydrophobicity measurements, the contact angle (Θ_c) of the water drop on the membrane surface was carried out using an optical tensiometer instrument (Biolin Scientific, Sweden) sessile drop method. 5 μL of water was used as a sessile drop on a dry membrane sample with 2.0 cm (width) × 4.0 cm (length) dimension and contact angle values were recorded within 5 s using a Hamilton syringe. To minimize error, the measurement was repeated ten times on each sample and then the average values were recorded.

Mechanical strength (ultimate tensile strength and strain-at-break) of PES and PES-AgNPs membranes were evaluated using a tensile testing machine (Tinius Olsen-H5KT, USA). Three samples of each membrane with a thickness of ~200 μm and a dimension of 2.0 cm (width) × 4.0 cm (length) were tested for the tensile test with gauge length set at 20 mm and the average values were reported.

Membrane porosity was determined according to a dry and wet weight method as reported in the literature [16,26]. The membrane pieces were immersed in water for 48 h and the overall porosity was estimated through the following Eq. (1).

$$\varepsilon(\%) = \left(\frac{\frac{(W_w - W_d)}{\rho_{H_2O}}}{\frac{(W_w - W_d)}{\rho_{H_2O}} + \frac{W_d}{\rho_{PES}}} \right) \times 100 \quad (1)$$

where ε is the porosity of membrane, W_w and W_d are the weights (g) of membranes in the wet and dry state, respectively, ρ_{H_2O} is the density of pure water (1.0 g cm^{-3}) and ρ_{PES} is the density of the membrane in a dry state.

Also, the mean pore radius was calculated using the filtration velocity method by the Guerout–Elford–Ferry equation [16].

$$r_m = \sqrt{\frac{(2.9 - 1.75\varepsilon) \cdot 8\mu l Q}{\varepsilon \cdot A \cdot \Delta P}} \quad (2)$$

where r_m is the mean pore radium (nm), ε is the membrane porosity, μ is the water viscosity (Pa·s), L is the membrane thickness (m), Q is the volume of permeated water per unit time (m^3 s^{-1}), A is the area of the membrane (m^2), and ΔP is the operating pressure (Pa).

The stability of AgNPs within the membrane matrix was studied by using an immersion technique [13]. Under continuous magnetic stirring, then cutting pieces of nanocomposite membranes were submerged in pure water (100 mL) for 6 d at ambient temperature (~23°C ± 2.0°C). The possible AgNPs leaching from the membrane was quantified using inductively coupled plasma-optical emission spectroscopy (ICP-OES, Perkin Elmer, USA) with plasma configuration model optima 8000.

2.4. Membranes performance investigations

In this work, pure water flux, removal of HA and BSA, and fouling tests of the prepared membranes were investigated using the stirred dead-end cell (01730, Amicon Model 8200, Millipore MA, Manufacturer: MilliporeSigma™ Germany) with an active membrane surface area of 28.7 cm^2 and total volume capacity of 180 mL. The cell was connected to a nitrogen gas cylinder for controlled pressure where operating pressure was set at 1.0 bar. The stirrer speed was controlled by a magnetic bar stirrer underneath the cell (Fig. 1). A constant stirring speed of 500 rpm was used in

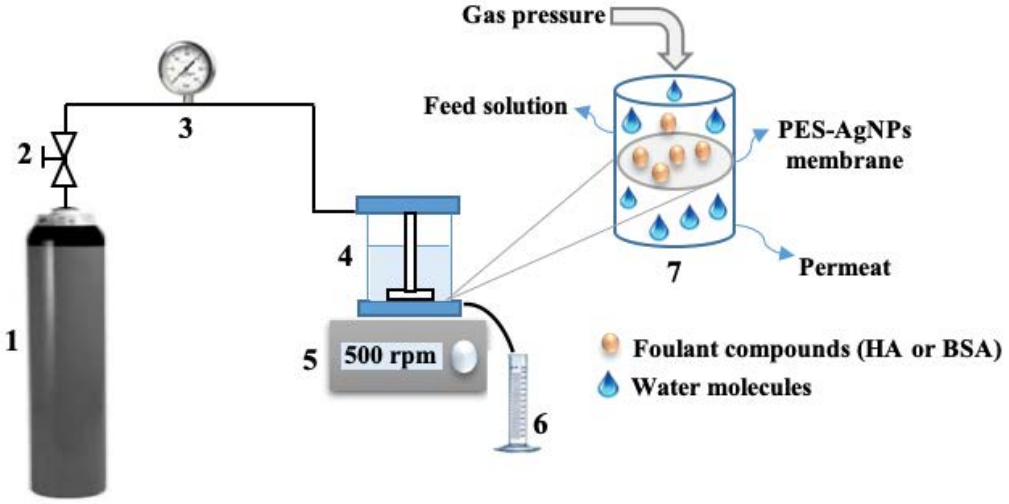

Fig. 1. Schematic diagram of the experimental apparatus: stirred dead-end cell set up a system (Amicon Model 8200): (1) gas cylinder (nitrogen), (2) pressure controller, (3) pressure gauge, (4) dead-end module, (5) magnetic stirrer, (6) graduated cylinder, (7) transport inside a dead-end module.

all membrane performance experiments. The neat PES and PES-AgNPs membranes were first compacted for 90 min at 2.0 bar to achieve a stabilization state. The permeate was collected each 15 min for 90 min and the pure water flux was estimated using Eq. (3) [15,27].

$$J = \frac{V}{A \times \Delta t} \tag{3}$$

where J is the flux (L m^{-2} h^{-1}), V is the volume of the collected permeate (L) at the period Δt (h), and A is the effective area of the membrane (m^2).

Two models of foulant compounds (HA and BSA) were used in this study to evaluate the rejection performance of the membranes. Humic acids were chosen as the model of natural organic compounds (10 ppm). First, the UF experiment was conducted with the HA solution (pH ≈ 8.4). The membrane rejection R (%) at feed conditions was then calculated using Eq. (4) [15,27].

$$R(\%) = \frac{C_F - C_P}{C_F} \times 100 \tag{4}$$

where C_F and C_P are the concentration of the feed and permeate solution (ppm), respectively. The experiment was repeated for the BSA solution (100 ppm). The concentrations of samples in permeate was determined using the calibration curve obtained from UV-Visible spectrophotometer (DR5000, Hach) measurement. This calibration curve was used for estimating unknown concentrations in each permeate during the experiment at the optical absorbance wavelength peak of λ_{254} nm for HA and λ_{279} nm for BSA. All the filtration tests were carried out three times and the average values were reported.

2.5. Organic antifouling properties

Cleaning is an important step in membrane processes since it has a substantial effect on process productivity. To measure the membrane pure water flux recovery (PWF_R), the used membranes were cleaned with deionized water for 15 min to remove the deposited BSA molecules. PWF_R is an index of the antifouling property of membranes and is used to compare the membrane water flux after cleaning (J_R) with the original membrane water flux (J_0) under the same operating condition by using Eq. (5) as shown below.

$$\mathrm{PWF}_R(\%) = \frac{J_R}{J_0} \times 100 \tag{5}$$

To study the effect of AgNPs on the membranes fouling, the BSA flux was measured and recorded as J_p. The fouling-resistant capacity of the membrane was quantified using Eqs. (6)–(8) [28].

$$R_t(\%) = \left(1 - \frac{J_P}{J_0}\right) \times 100 \tag{6}$$

$$R_r(\%) = \left(\frac{J_R - J_P}{J_0}\right) \times 100 \tag{7}$$

$$R_{\mathrm{ir}}(\%) = \left(1 - \frac{J_R}{J_0}\right) \times 100 \tag{8}$$

where R_t, R_r, R_{ir} are total fouling, reversible fouling, and irreversible fouling, respectively.

2.6. Antibacterial activity of membranes

The antibacterial activity of resultant PES-AgNPs nanocomposite membranes was tested using the Gram-positive bacterium *B. subtilis* (SQUMSF005) and Gram-negative bacterium *E. coli* (ATCC 25922) under dark and visible light environment. Prior to the test, both bacterial strains were cultivated for 24 h in Luria Bertani (LB) medium at 37°C ± 1.0°C. In total three different treatments were used, such as LB broth without bacteria (blank control), LB broth with bacteria but without membrane (bacterial control), and LB broth with bacteria and different PES-Ag nanocomposite membranes. The sections 1.0 cm × 1.0 cm were cut from each membrane. Each membrane was placed at the bottom of each well of the 12-well plate (Costar, Tewksbury, MA, USA). The replicates for each membrane were used. Each well was filled with 3.0 mL of a broth culture of the bacterium. In parallel, the same type of experimental setup was prepared and covered with aluminum foil and then used as a dark condition test. Every 24 h for two consecutive days, 100 mL of the broth culture from each well was collected and transferred into a sterile 96-well microtiter plate (Nunc, Denmark). The optical density (OD) absorbance of the collected samples in the plate was measured using a plate reader device (Thermo, USA) at a wavelength λ of 620 nm (OD_{620}). Then, the mean value and standard deviation of three replicates for each membrane were calculated.

In order to estimate the number of alive bacteria, the number of colony-forming units (CFU) was calculated [Eq. (9)]. Briefly, in order to do this a serial dilution of an original sample was done. Then, 0.1 mL of the diluted sample was plated on a petri dish containing sterile nutrient agar (Difco, USA). The plates were incubated for 24 h at 37°C ± 1.0°C. Finally, the number of colonies was counted manually.

$$\frac{\mathrm{CFU}}{\mathrm{mL}} = \frac{\text{Number of colonies} \times \text{dilution factor}}{\text{Plate volume}(\mathrm{mL})} \tag{9}$$

3. Results and discussion

3.1. Membranes characterization

3.1.1. Morphological studies

The FE-SEM images of prepared membranes by varying the AgNPs loading are shown in Fig. 2. From the top surface morphology, a slight change in the surface roughness of membranes was observed due to the inclusion of AgNPs. No significant accumulation of AgNPs was witnessed which revealed good miscibility of AgNPs in the polymer matrix, especially for lower AgNPs content (0.5 wt.%). Addition of 2.0 wt.% of the nanoparticle into PES showed the agglomeration of nanoparticles on the membrane surface. This can be attributed to the poor dispersion of higher nanoparticle addition.

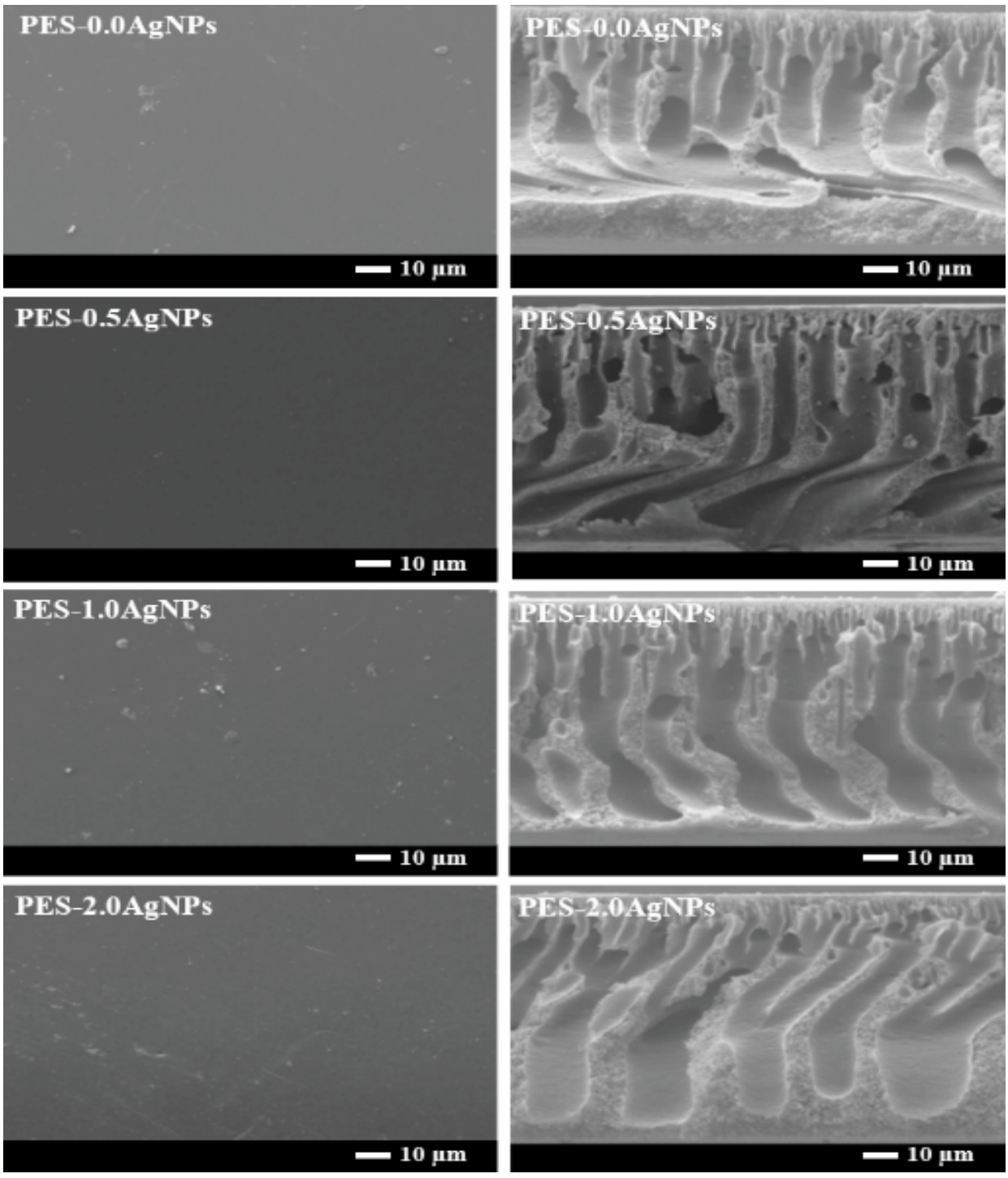

Fig. 2. FE-SEM images of membranes: (left) top surface, (right) cross-sectional.

As the loading percent of AgNPs increased from 0.5% to 2.0%, the viscosity of the polymer solution increased as well (Table S1 and Fig. S1). The elevation of PES-AgNPs solution viscosity slower the water-solvent exchange rate. The solutions viscosity stayed constant with increasing applied shear rate which indicates all dope solutions follow Newtonian behavior. This might induce specific changes in membrane morphology which in turn would affect the porosity, macro-void formation, and also permeability of membranes.

In general, the cross-sectional images of membranes exhibit the typical asymmetric structure, consisting of a top dense skin layer (selective layer) near the top surfaces followed by a thick finger-like with macrovoids (sub-layer), and sponge-like (bottom layer). The pristine membranes

(PES-0.0AgNPs) revealed blocked pore channels with thin macrovoid in the center of the membrane sublayer. Our findings were similar to those reported by Thuyavan et al. [1] for the unmodified PES membranes. In contrast, the cross-sectional structures were partially changed when the AgNPs loads into the membranes. All modified membranes showed quite similar morphology and the finger-like structures have elongated and become wider at the bottom as compared to the control membranes (PES-0.0AgNPs). This distribution of the pores and channels could provide better membrane performance in terms of permeability and probably effect on rejection tests. These differences in morphological characteristics between PES and PES-AgNPs membranes might be due to two main reasons: first, the exchange rate of non-solvent (water) and solvent (NMP) through the phase inversion process. Both thermodynamic phase equilibrium and kinetic aspects play a role during the phase inversion technique. The hydrophilic nature of the AgNPs in the polymeric solution can increase both the solution thermodynamic instability in the coagulation bath and the mass transfer rate between the NMP solvent and water. Consequently, the exchange rate affects change in the membranes morphology and pore formation due to promoting a fast phase inversion [25,29]. Second, increased the casting solutions hydrophilicity was induced by the hydrophilic AgNPs [30].

Energy-dispersive X-ray spectroscopy was used to determine the percentage elemental composition of PES and PES-AgNPs membranes (Fig. S2). The weight percentage of AgNPs increased as the loading concentration of AgNPs increased in the casting solution. Due to the specific area detection of Ag element on the sample surface, there was some discrepancy in wt.% of Ag element. For instance, the initial silver composition in the mixed solution of PES-0.5AgNPs was found to be 0.45 wt.%, for PES-1.0AgNPs sample surface showed 0.80 and 1.90 wt.% for PES-2.0AgNPs nanocomposite membranes, respectively.

3.1.2. XRD analysis

The crystallinity of the resultant nanocomposite membranes was also confirmed by XRD and the results are shown in Fig. 3. Silver peaks were found to be more noticeable in the samples with increasing nanoparticle content. At $2\theta = 18.1°$, a broad peak appears in the case of PES-0.0AgNPs indicating the amorphous structure of PES polymer found from the aromatic benzene ring (C_6H_6) and the flexible ether bond (R-O-R′) structure. The main diffraction due to AgNPs crystals occurs at 27.184°, 31.84°, 37.68°, 44.016°, 46.016°, 64.176° and 77.008° which are indexed to (210), (122), (111), (200), (231), (220) and (311) planes of pure silver based on the face-centered cubic structure (JCPDS No. 04-0783 "Joint Committee on Powder Diffraction Standards") [13].

3.1.3. ATR-FTIR analysis

The ATR-FTIR spectra of the PES and PES-AgNPs membranes were carried out to identify the functional groups present on the membrane surfaces. Fig. 4 displays the main functional groups exhibited by membranes which are C=C, C–C, S=O and C–O–C/C–O. All FTIR spectra for Ag incorporated membranes are similar to PES-0.0AgNPs membrane patterns and no additional peaks were detected upon the addition of AgNPs due to the same chemical composition content in the prepared dope solutions. The PES structure corresponding peaks appear at the wavenumber of 1,579.4 cm^{-1} obtained from the C=C stretching vibration

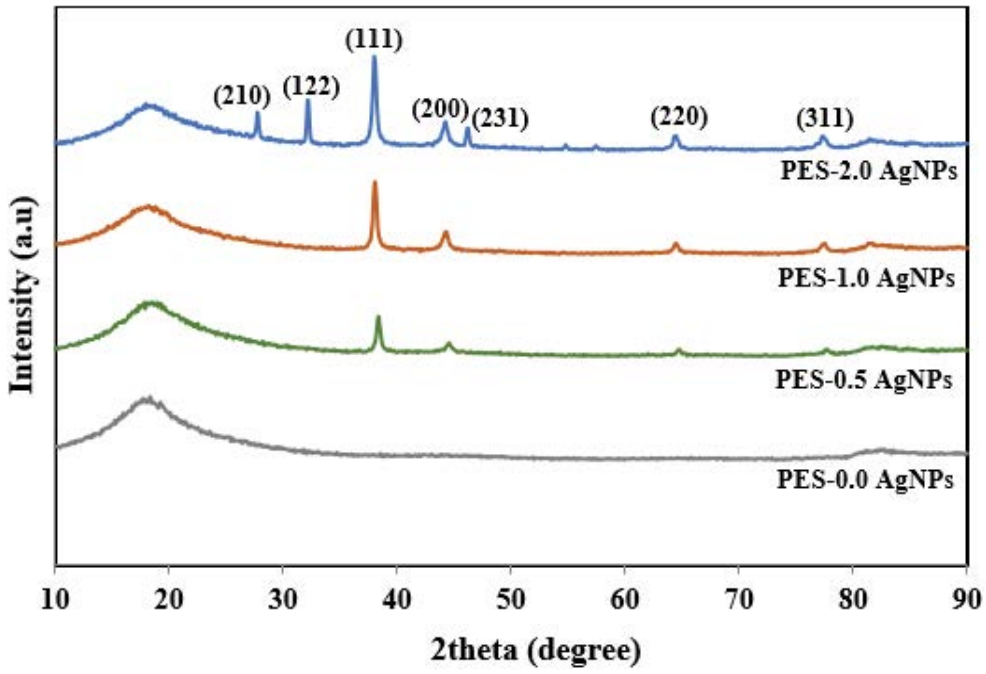

Fig. 3. XRD spectra of PES and PES-AgNPs nanocomposite membranes.

of benzene rings. The peak presence in the range of 1,490; 1,104.8; 1,243.4 cm^{-1} indicates the presence of the C–C band of the aromatic ring, aromatic ether C–O–C/C–O band and sulfone group (S=O), respectively. Thus, it can be reasonably concluded that the inclusion of AgNPs does not affect the molecular integrity of the PES membranes.

3.1.4. Surface wettability

Contact angle measurements were evaluated to determine the changes in PES membrane's surface hydrophilicity upon inclusion of AgNPs (Fig. 5). The highest WCA was observed for pure PES (PES-0.0AgNPs) with a WCA

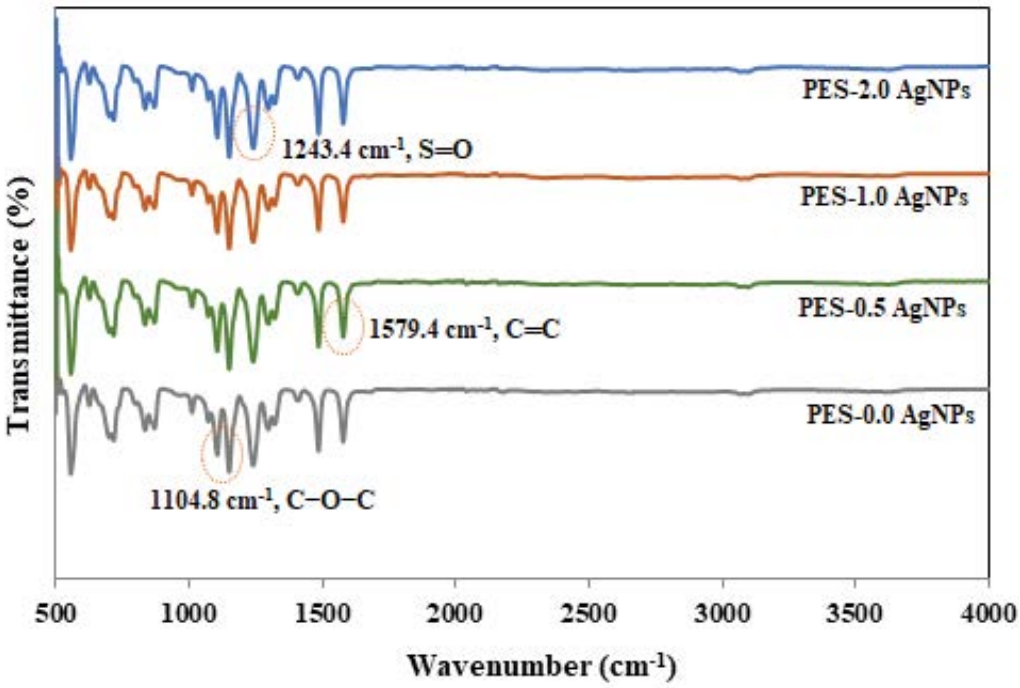

Fig. 4. ATR-FTIR spectra of PES and PES-AgNPs nanocomposite membranes.

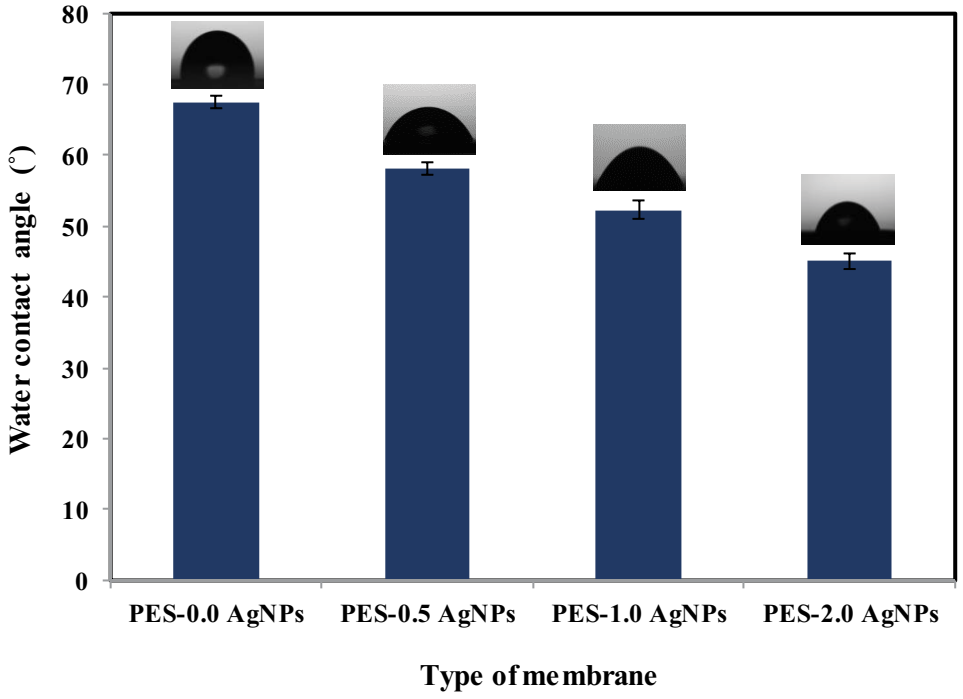

Fig. 5. Water contact angle values of the PES and PES-AgNPs nanocomposite membranes were measured at ambient temperature.

value of 68 ± 1.0°. The PES polymer has low hydrophilicity due to the intrinsic nature of the hydrocarbon compound. Compared to the pristine PES membrane, the addition of AgNPs improved the membrane hydrophilicity in which the contact angle of the nanocomposite membrane dropped gradually from 68 ± 1.0° (pure PES) to 58 ± 1.0°, 52 ± 1.0° and 45 ± 1.0° with increasing content of AgNPs from 0.5, 1.0, to 2.0 wt.%, respectively. The highest loading of AgNPs (2.0 wt.%), has resulted in an improvement in the fabricated membrane surface (better hydrophilicity). Our findings are similar to those reported in the literature, who used synthetic AgNPs in the range of 0.32–2.0 wt.% and reported enhanced fouling resistance and water flux of polymeric membranes [15,16]. The presence of the AgNPs within the membrane structure can lead to the increment of interface surface energy and lower the surface tension of PES membranes. Consequently, the adhesive forces that exist between the water molecules and membrane surface will be higher than cohesive forces that exist between the water molecules. As a result, a reduction in the contact angle was due to form strong water molecules bonding to the membranes surface rather than attraction to each other which improves the membrane water flux (Section 3.2.1 – Measurement of water flux, HA and BSA rejection).

3.1.5. Membrane porosity

The most important characteristics of semipermeable membranes are total porosity and pore radius, which determines their productivity and selectivity as shown in Table 1 the porosity and pore radius of the pristine PES and PES-AgNPs modified membrane. The addition of AgNPs increased the membrane porosity from 63% for pure PES to 86% for PES-2.0AgNPs membrane. Regarding the membrane pore size, it is observed that the pore size of the PES-0.0AgNPs membrane is slightly increased from 19.03 to 21.41 nm upon loading with 0.5 wt.% of AgNPs. Generally, the pore formation of membranes can be linked to pore formation during the polymeric membrane fabrication process. Adding AgNPs into dope solution can weaken the interaction forces that exist between NMP solvent and the polymer (reduces the thermodynamic stability of the dope solution). This result may be a fast exchange rate between NMP solvent molecules and water molecules during the phase inversion process due to the hydrophilic property of AgNPs [16]. As a result, the formation of larger pore size and porosity structure of the polymeric membrane due to leaching of agglomerated nanoparticles during fabrication process especially at higher AgNPs loading (Section 3.1.7 – Silver release) [25,26]. This clarified the main reason that the PES-2.0AgNPs membrane exhibited the highest bulk porosity and pore size with the maximum water flux among others membranes.

Table 1
Pore structure parameters of PES and PES-AgNPs modified membranes

Membranes code	Bulk porosity (%)	Pore radius (nm)
PES-0.0AgNPs	63.35 ± 0.35	19.03 ± 0.21
PES-0.5AgNPs	71.21 ± 0.59	21.41 ± 0.52
PES-1.0AgNPs	78.14 ± 1.07	26.11 ± 0.10
PES-2.0AgNPs	86.02 ± 0.09	29.40 ± 0.31

3.1.6. Mechanical strength

The mechanical properties of the fabricated membranes were evaluated with respect to true stress-true strain curve as shown in Fig. S3. The mechanical strength improved up to 55% of 0.5 wt.% AgNPs loading when compared to pristine PES. However, a further increase of the AgNPs loading up to 2.0 wt.%, dropped the tensile strength by 43.87%.

The brittleness of the pristine membrane and PES-AgNPs modified membranes were studied also in terms of tensile strength and elongation at break as shown in Fig. 6. Elongation at the breaking point increased from 4.1% for pristine PES (PES-0.0AgNPs) to 8.5% for the PES-0.5AgNPs membrane. When AgNPs loading was increased, the % reduction in elongation was observed. A similar observation was observed where the young's modulus increased from 120 MPa for pristine PES to 266.67 MPa for the PES-0.5AgNPs. When AgNPs were incorporated into the PES membrane, the interaction between AgNPs and polymer matrix increased and consequently, improved the interfacial viscoelastic deformation in PES-AgNPs composite membrane. Besides, both yield strength and ultimate strength increased from 4.4 MPa (pristine PES) to 5.5 MPs and from 1.7 (pristine PES) to 2.7 MPa when incorporating 0.5 wt.% AgNPs to PES (Fig. 6b). Then both parameters decreased gradually with increasing content of silver nanoparticles in PES membranes.

This phenomenon occurs because when more AgNPs were added to the PES, Ag nanoparticles seemed to agglomerate and lower the nanoparticle's dispersion within the polymer matrix. In addition, under testing conditions, large macro-voids were filled with air and reduced the compactness (longer finger structure). Thus, the membrane tensile strength may decrease due to the present of pores [26]. Mostly, longer elongation and higher tensile strength are associated with the tight interior structure and dense skin of the membranes. The membrane is more ductile and does not easily damage despite being given a heavier workload. The results indicate that the reduction in the tensile strength leads to an increase in the water content and porosity of the membranes as evidenced by the membrane porosity in (Section 3.1.5 – Membrane porosity) and water flux results.

3.1.7. Silver release

Detection for silver leaching was carried out to investigate the strength attachment of AgNPs within the membrane matrix. From Table 2, the PES-0.5AgNPs nanocomposite membranes only suffered from minimal AgNPs leaching in comparison to the other two membranes as expected since both PES-1.0AgNPs and PES-2.0AgNPs were loaded with more AgNPs and most of the nanoparticles were agglomerated on the membranes surface without integrating with membranes matrix (poor adhesion to the

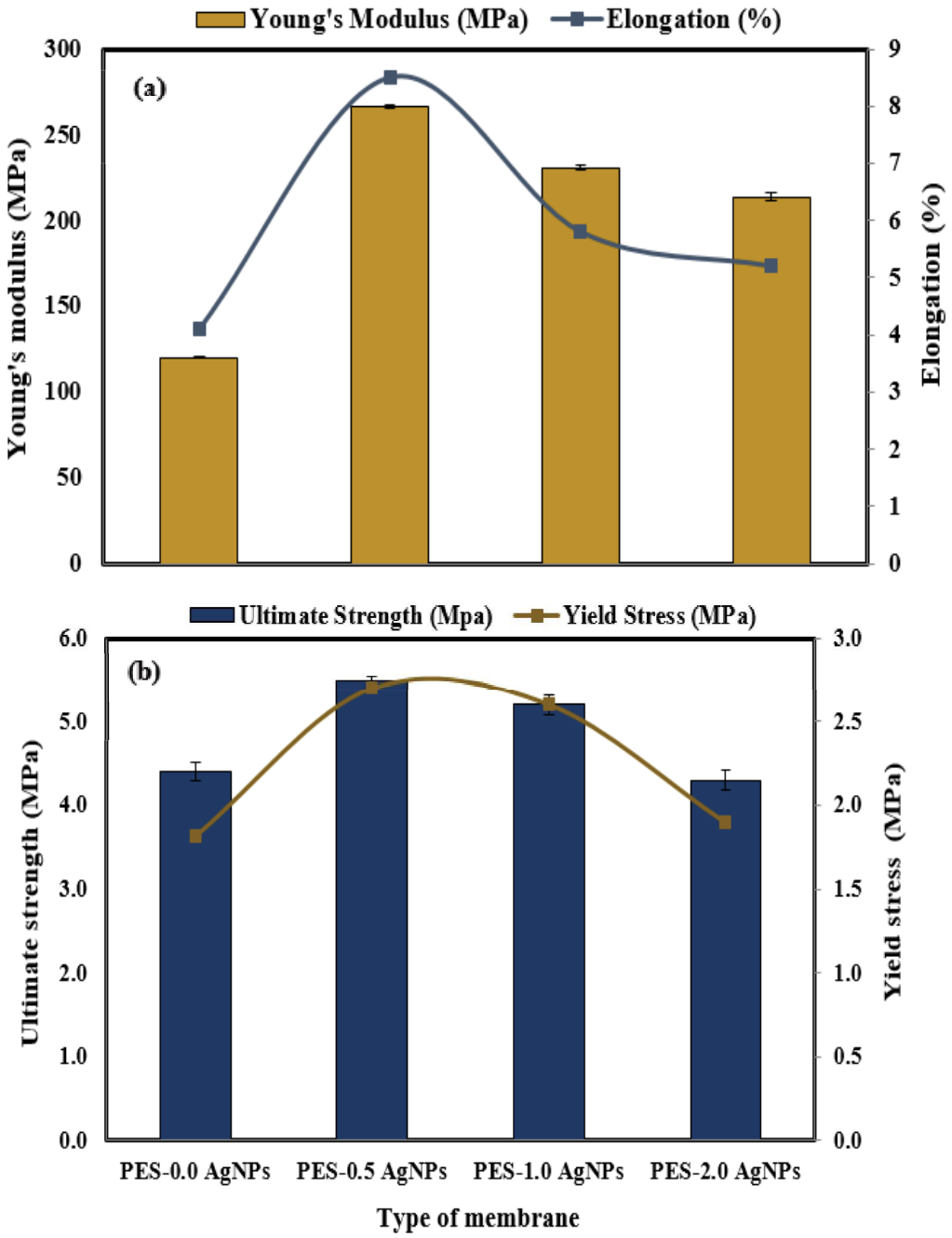

Fig. 6. (a) Tensile strength and elongation-at-break of PES and PES-AgNPs membranes and (b) ultimate strength and yield strength of PES and PES-AgNPs membranes.

Table 2
Detection of AgNPs element by ICP-OES for different PES-AgNPs nanocomposite membranes during 6 d

Membranes code	Ag element detected (mg g^{-1} of membranes)
PES-0.5AgNPs	0.0136 ± 0.0018
PES-1.0AgNPs	1.4540 ± 0.0483
PES-2.0AgNPs	4.6357 ± 0.0188

PES matrix). Usually, a high release of silver from the composite membrane is good for antimicrobial activity and antigrowth of bacteria (Section 3.3.2 – Biofouling properties) as reported by others [23,31]. On the other hand, the rapid depletion of silver in the membrane reduces the strength and membrane's lifetime [13]. According to the world health organization (WHO), the secondary maximum contaminant level of silver ions in drinking water is 100 ppb or 0.1 ppm [13,32]. All leaching studies performed with high AgNPs loading (PES-1.0AgNPs and

PES-2.0AgNPs) would have been unsuccessful to conform to drinking water regulations in comparison to the PES-0.5AgNPs membrane was not in the hazardous level. Control release of AgNPs can be improved either by incorporation of a capping agent [16] or functionalized the polymer [13]. These are the most common strategies that could improve particles dispersibility, prevent agglomeration of AgNPs and stabilize AgNPs in the polymeric membrane matrix with better membranes performance.

3.2. Membranes performance

3.2.1. Measurement of water flux, HA and BSA rejection

The fabricated membranes were evaluated for their performance in terms of pure water flux, HA and BSA rejection. It was observed that the pure water flux initially increased with further increments of AgNPs in the casting solution (Fig. 7a). PES-2.0AgNPs show the highest flux of 14.19 ± 0.12 L m^{-2} h^{-1} while pristine PES membrane had the lowest flux of 1.76 ± 0.05 L m^{-2} h^{-1} indicating a 12.43% improvement in the permeability of the membrane. This enhancement in water flux of the modified PES membranes can be explained as follows: First, membrane's hydrophilicity property was improved after adding nanoparticles due to silver hydrophilic nature which could attract water molecules inside the membrane matrix and promote them to pass through the membrane (Fig. 5). Second, agglomeration of silver NPs tended to enlarge the membrane pores (especially at higher NPs loading) while leaching of these agglomerated AgNPs during phase inversion would

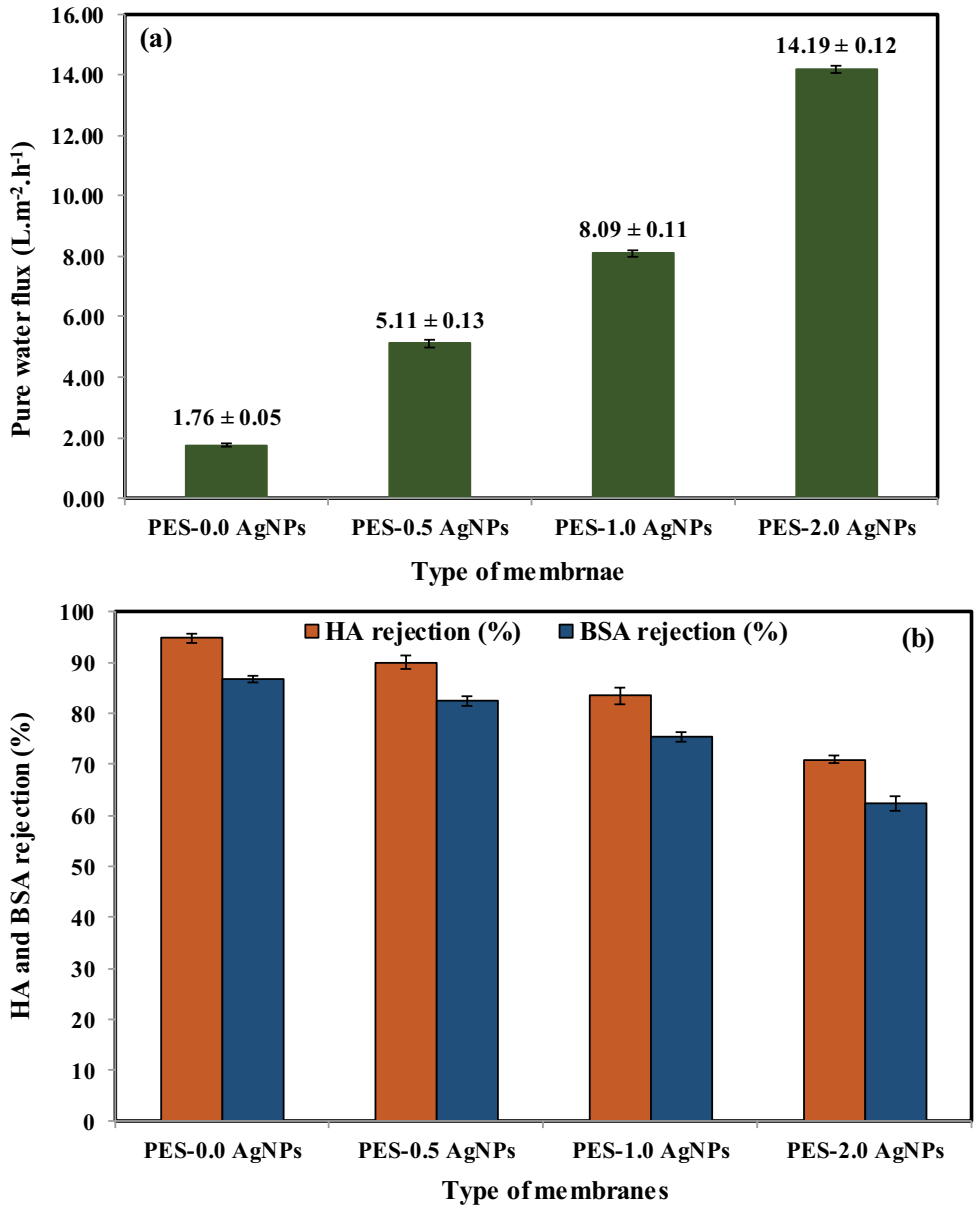

Fig. 7. (a) Average pure water flux of PES and modified PES-AgNPs nanocomposite membranes and (b) rejection of protein and organic pollute of PES and modified PES-AgNPs nanocomposite membranes.

leave the membrane with higher porosity and pore size (Table 1). This explained why membrane with 2.0 wt.% AgNPs loading displayed the largest membrane porosity with the highest PWF among other membranes. Third, the reason might be also related to different membrane cross-section structures (Fig. 2). Specifically, AgNPs performed as pore formers on the membranes to build more various small water channels in the membranes cross-sections [33]. Thus, the water flux of membranes increased with the addition of AgNPs. Similar findings were reported by Dong et al. During the filtration study, the average flux values of pure cellulose acetate membranes were determined to be 11 L m^{-2} h^{-1}, while membranes embedded with AgNPs showed significant increases in flux to 18 and 25 L m^{-2} h^{-1}, with increasing amounts of AgNPs from 1.0 to 2.0 wt.%, respectively. This is likely due to the AgNPs acting as pore formers [33].

With respect to separation performance, the rejection efficiency of a membrane depends strongly on the membrane structure, molecular volume, and the physicochemical characteristics of the feed solution properties. Individually UF test was performed with the HA and BSA solution and the results are shown in Fig. 7b. The rejection of the pristine PES-0.0AgNPs membrane was 94.72% and 86.72%, for the HA and BSA solution, respectively. As the AgNPs content increase in the PES solution, the percentage rejection decreased to 70.99% for HA and 62.30% for BSA at 2.0 wt.% of AgNPs concentration. The decrease in rejection with increasing AgNPs concentration can be explained as increased porosity of the membranes during the fabrication process as explained previously (Section 3.1.5 – Membrane porosity), which increases its capability towards low rejection and low obstacle membrane structure as clear from FE-SEM images (Fig. 2). Among all, membranes loading with fewer AgNPs concentrations (0.5 wt.%) is preferable to achieve high rejection efficiency with low pure water flux compared to high AgNPs loading (1.0 and 2.0 wt.%). Where the porosity of PES-0.0AgNPs membrane was approximately 26% smaller than PES-2.0AgNPs membranes. Consequently, the rejection of organics by the pristine membrane was better than membranes at higher AgNPs loading. Results showed that the fabricated PES membranes rejected the organic matter effectively based on size exclusion mechanism. These results are in agreement with other findings that have been reported in the literature, who fabricated PES membranes incorporated with $AgNO_3$ (0.5 and 2.0 wt.%). The authors reported the membrane porosity increased with a higher Ag loading in the membrane. The presence of Ag had increased the membranes pore size average from 0.047 μm for pristine PES membranes to 0.213 μm for PES-Ag2.0 [16]. In contrary, some researchers reported that higher Ag content lead to reduced membrane pore size, resulting in a lower permeability but better solute rejection [29]. Overall, rejection of HA and BSA molecules would be increased with a decrease in membrane bulk porosity and pore size as one of the most significant parameter effect on membrane performance and enhance organic matter removal as reported in literature [14,16,29]. Compared to HA rejection, BSA rejection was less as the AgNPs loading increases due to its lower protein molecular weight (less BSA macromolecules) resulting in lower rejection by the size exclusion effect of the membrane.

3.3. Membrane fouling

3.3.1. Anti-organic fouling performance

In this work, BSA was selected as the fouling substance to evaluate the antifouling performance of the membrane. After cleaning the membranes with deionized water, the membranes flux recoveries were measured, and the results are presented in Fig. 8a. It is observed that flux recoveries improved from 71.12% for PES-0.0AgNPs membrane to 97.29% for modified PES-2.0AgNPs membrane. The main reason for improvement of flux recoveries resulted from the enhanced membranes surface hydrophilicity after loading the AgNPs which assist the formation of a hydrated layer of hydrogen bonding with water molecules that prevent firm adhesion of the foulants on the membrane surfaces. This means in the case of the modified membrane, foulants were adsorbed only at the membrane surface that can be easily removed by simple washing [1].

The BSA antifouling parameters (R_t, R_r and R_{ir}) were predicted from the initial water flux, the BSA flux and the recovery flux. The calculated fouling probabilities are presented in Fig. 8b. The total fouling of unmodified PES membrane was found to be higher than modified membranes. The results revealed that the irreversible resistance of the PES membrane was the main part of the total fouling. The irreversible fouling is due to adsorption of BSA molecules on the surface or entrapment of BSA molecules in pores while reversible fouling arises from reversible protein adsorption which can be removed by simple washing. For nanocomposite membranes, the irreversible fouling was sharply reduced with the minimum value of 3.7% for PES-2.0AgNPs. The improved antifouling performance of the nanocomposite membranes was attributed to a combination of factors such as hydrophilic nature of membranes surface and the lower roughness of the membrane surface. Increasing AgNPs composite increased hydrophilicity of the surface as observed from WCA results (Fig. 4). This increased hydrophilicity is led to reducing the interaction of BSA with the membrane surface.

3.3.2. Biofouling properties

AgNPs is a well-known as an anti-bacterial agent against a wide range of microorganisms [11,16,17]. In this work, both Gram-positive (*B. subtilis*) and Gram-negative (*E. coli*) bacteria were used to investigate the antimicrobial property of the PES-AgNPs nanocomposite membranes. The bacterial growth of *B. subtilis* under the light and dark conditions is shown in Figs. S4 and S5, correspondingly. Similarly, the bacterial growth of *E. coli* under the light and dark conditions is shown in Figs. S6 and S7, respectively.

For *B. subtilis*, there was a significant reduction in bacterial abundance compared to the control (PES-0.0AgNPs) under the light condition. In both bacteria, maximum reduction in absorbance was observed for PES membranes modified with 1.0 and 2.0 wt.% AgNPs after 48 h. The reduction of bacterial growth was found for all PES-AgNPs samples, while incubation time is increased. However, for the control

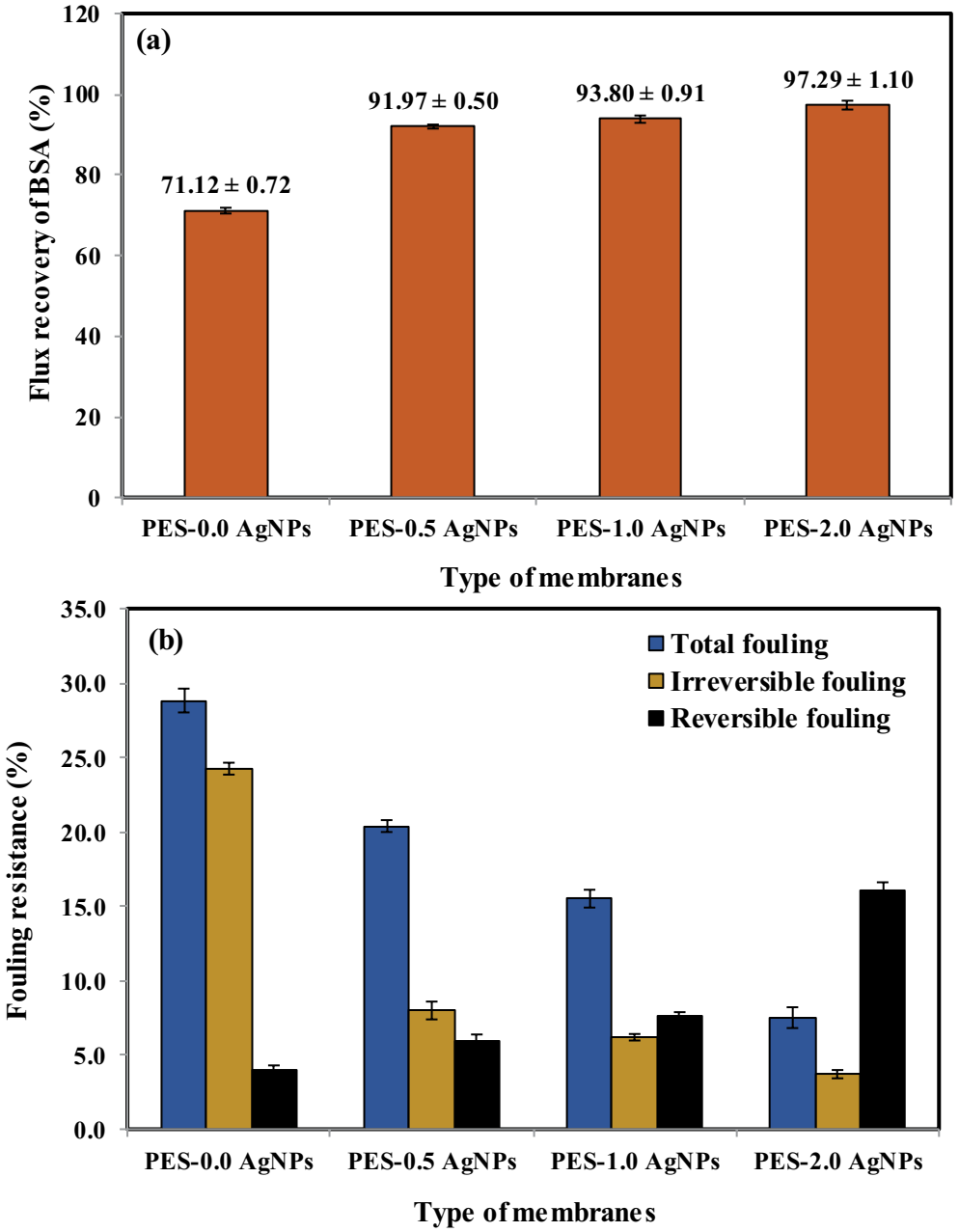

Fig. 8. (a) Pure water flux recovery after BSA filtration measure at 1.0 bar for the PES and AgNPs- modified membranes and (b) fouling BSA resistance parameters of PES and PES-AgNPs nanocomposite membranes.

sample (PES-0.0AgNPs) after 48 h, the bacterial re-growth was significant (Fig. S4a). Under the dark condition, bacterial re-growth was very similar for the control sample (PES-0.0AgNPs). In general, the bacterial growth was lower for PES-AgNPs nanocomposite membranes which indicate that most of the bacteria killed with the modified membranes due to antibacterial activity of AgNPs. Among PES-AgNPs nanocomposite membranes, a low concentration of AgNPs sample (PES-0.5AgNPs) was experienced slight re-growth of bacteria. PES-1.0AgNPs and PES-2.0AgNPs samples showed constant bacterial growth throughout 48 h (see the black arrow for the reference in Fig. S5). The highest antibacterial activity of 50% was achieved with the PES-2.0AgNPs membrane within 48 h.

Under the light condition, the control sample showed re-growth of *E. coli* bacteria for 48 h (Fig. S6). But for PES-AgNPs nanocomposite membranes, slight decrement of *E. coli* bacteria at the first 5 h of incubation time followed by substantial decrease in optical density of bacteria was observed over 48 h. For PES-2.0AgNPs samples, 99.1% of the bacteria were inactivated within 48 h (shown with a red arrow in Fig. S6a). Interestingly, bacterial re-growth was observed for the control and PES-AgNPs nanocomposite membranes under the dark condition within 48 h of incubation time

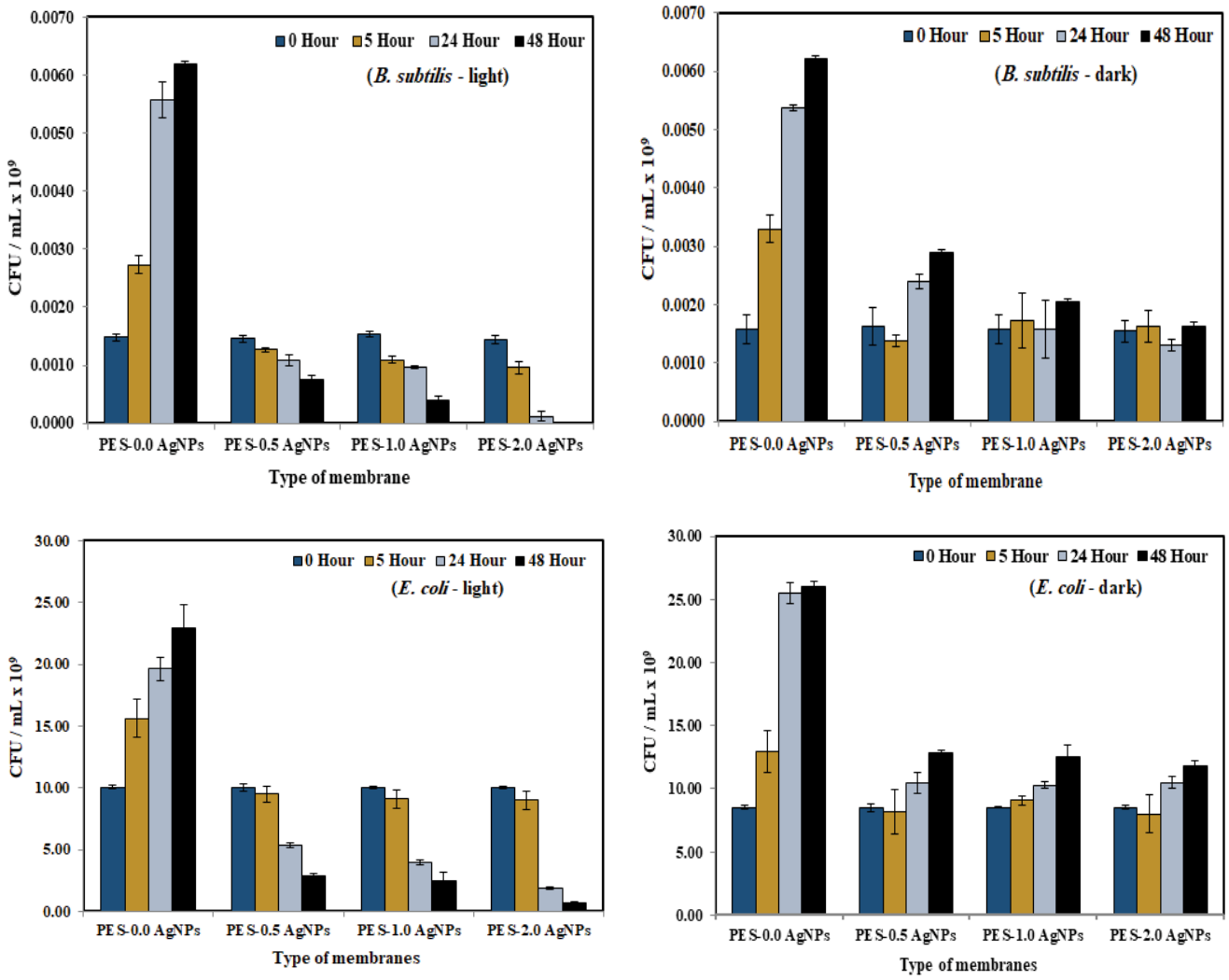

Fig. 9. Effect of PES-AgNPs membranes in the light (30–35 W m^{-2}) and dark (0 W m^{-2}) conditions on colony-forming units (viable cells) for bacteria of three replicates.

(Fig. S7a). As expected, the control sample has the highest bacterial growth compare with nanocomposite membranes. Among PES-AgNPs nanocomposite membranes, low concentration of AgNPs membrane (PES-0.5AgNPs) showed the highest bacterial growth and the lowest growth was witnessed for PES-2.0AgNPs membrane. Thus, it can be concluded that visible light activation of pure PES and PES-AgNPs nanocomposite membranes was played an important role in antibacterial activity. Additionally, release of Ag^+ ions from the membrane under the light conditions could be higher compare to the dark, which could contribute to the higher antibacterial activity. For the light activation process, PES-2.0AgNPs membrane inactivated 50% of the Gram-positive *B. subtilis* but 99.1% was achieved for Gram-negative *E. coli*. Thus, fabricated PES-AgNPs nanocomposite membranes were highly selective for Gram-negative bacteria. This could be explained by the difference in cell wall between Gram-positive and Gram-negative bacteria [34].

In order to confirm that bacteria were inactivated by the membranes, the number of CFU was counted under the light and dark conditions (Fig. 9). The CFU results were in a good agreement with the previously reported OD measurement results. Under the light condition, PES-AgNPs nanocomposite membranes reduced CFU drastically but re-growth trend was observed under the dark conditions for both *B. subtilis* and *E. coli* bacteria within 48 h. In contrast, *B. subtilis* CFU count showed 100% inactivation, while OD measurements were two folds higher. The difference between OD and CFU results could be explained by the interference of the dead bacteria during OD measurement. Experiments with the Gram-negative *E. coli* showed 83% reduction of CFU.

Overall, our experiment demonstrates the following: pure PES membrane did not inhibit growth of both bacteria under the light and dark conditions. Addition of silver into the membrane increased antibacterial activity. The strongest highest antibacterial activity was observed for the PES-2.0AgNPs membrane that contained the highest tested concentration of silver. Similarly, it was reported that increase in the amount of AgNPs in membrane would increase membrane antimicrobial activity [31,35]. Under the

light condition most of bacteria were killed suggesting that light increased the leaching of silver from the membrane thus increasing the antibacterial effect.

4. Conclusions

In the current study, PES membranes blended with silver nanoparticles were fabricated via phase inversion by the immersion precipitation technique based on different AgNPs loadings. As silver loading increased, the PES-AgNPs membrane's pore size and porosity increased. This resulted in higher PWF and lower HA and BSA rejection. On top of that, the antibacterial performance of the PES-AgNPs membrane was enhanced significantly at higher silver loading (2.0 wt.%) especially under light conditions, while the unmodified PES membranes did not exhibit any antibacterial property. The water contact angle results showed that hydrophilicity of the PES membrane increased along with silver loading, which was deemed to be advantageous in preventing the membrane from organic fouling. In brief, the incorporation of AgNPs in PES membranes justified the potential in treating wastewater owing to its enhanced membrane surface hydrophilicity, permeability, antifouling ability, and antibacterial property. PES-2.0AgNPs membrane showed the optimum flux and antibacterial performance among other membrane samples despite a slight reduction in HA and BSA rejection which was acceptable.

Conflicts of interest

The authors declare no conflict of interest

Acknowledgments

The authors of this work would like to thank Nanotechnology Research Center at Sultan Qaboos University and the Institute for Nanotechnology and Water Sustainability in the University of South Africa for their financial support under grant numbers CL/SQU-SA/18/03.

References

[1] Y. Lukka Thuyavan, N. Anantharaman, G. Arthanareeswaran, A. Fauzi Ismail, Impact of solvents and process conditions on the formation of polyethersulfone membranes and its fouling behavior in lake water filtration, J. Chem. Technol. Biotechnol., 91 (2016) 2568–2581.

[2] M. Al-Abri, B. Al-Ghafri, T. Bora, S. Dobretsov, J. Dutta, S. Castelletto, L. Rosa, A. Boretti, Chlorination disadvantages and alternative routes for biofouling control in reverse osmosis desalination, npj Clean Water, 2 (2019) 1–16, doi: 10.1038/s41545-018-0024-8.

[3] A. Abushaban, S.G. Salinas-Rodriguez, D. Pastorelli, J.C. Schippers, S. Mondal, S. Goueli, M.D. Kennedy, Assessing pretreatment effectiveness for particulate, organic and biological fouling in a full-scale SWRO desalination plant, Membranes, 11 (2021) 167, doi: 10.3390/membranes11030167.

[4] A.T. Besha, A.Y. Gebreyohannes, R.A. Tufa, D.N. Bekele, E. Curcio, L. Giorno, Removal of emerging micropollutants by activated sludge process and membrane bioreactors and the effects of micropollutants on membrane fouling: a review, J. Environ. Chem. Eng., 5 (2017) 2395–2414.

[5] X. Chen, Y. Su, F. Shen, Y. Wan, Antifouling ultrafiltration membranes made from PAN-b-PEG copolymers: effect of copolymer composition and PEG chain length, J. Membr. Sci., 384 (2011) 44–51.

[6] M. Zahid, A. Rashid, S. Akram, Z.A. Rehan, W. Razzaq, A comprehensive review on polymeric nano-composite membranes for water treatment, J. Membr. Sci. Technol., 8 (2018) 1000179, doi: 10.4172/2155-9589.1000179.

[7] B.S. Lalia, V. Kochkodan, R. Hashaikeh, N. Hilal, A review on membrane fabrication: structure, properties and performance relationship, Desalination, 326 (2013) 77–95.

[8] M. Zajda, U. Aleksander-Kwaterczak, Wastewater treatment methods for effluents from the confectionery industry – an overview, J. Ecol. Eng., 20 (2019) 293–304.

[9] G. Crini, E. Lichtfouse, Advantages and disadvantages of techniques used for wastewater treatment, Environ. Chem. Lett., 17 (2019) 145–155.

[10] X.M. Tan, D. Rodrigue, A review on porous polymeric membrane preparation. Part I: production techniques with polysulfone and poly(vinylidene fluoride), Polymers, 11 (2019) 1160, doi: 10.3390/polym11071160.

[11] B.A. Bolto, Z.L. Xie, Recent developments in fouling minimization of membranes modifed with silver nanoparticles, J. Membr. Sci. Res., 4 (2018) 111–120.

[12] X. Cui, K. Choo, Natural organic matter removal and fouling control in low-pressure membrane filtration for water treatment, Environ. Eng. Res., 9 (2014) 1–8.

[13] M. Salman Haider, G.N. Shao, S.M. Imran, S.S. Park, N. Abbas, M. Suleman Tahir, M. Hussain, W. Bae, H.T. Kim, Aminated polyethersulfone-silver nanoparticles (AgNPs-APES) composite membranes with controlled silver ion release for antibacterial and water treatment applications, Mater. Sci. Eng. C, 62 (2016) 732–745.

[14] A.L. Ahmad, A.A. Abdulkarim, B.S. Ooi, S. Ismail, Recent development in additives modifications of polyethersulfone membrane for flux enhancement, Chem. Eng. J., 223 (2013) 246–267.

[15] Z.A. Rehan, L. Gzara, S.B. Khan, K.A. Alamry, M.S. El-Shahawi, M.H. Albeirutty, A. Figoli, E. Drioli, A.M. Asiri, Synthesis and characterization of silver nanoparticles-filled polyethersulfone membranes for antibacterial and anti-biofouling application, Recent Pat. Nanotechnol., 10 (2016) 231–251.

[16] H. Basri, A.F. Ismail, M. Aziz, Polyethersulfone (PES)–silver composite UF membrane: effect of silver loading and PVP molecular weight on membrane morphology and antibacterial activity, Desalination, 273 (2011) 72–80.

[17] Y. Chen, X. Liu, L. Liu, Y. Zhang, Z. Wang, Q. Zhang, Functional poly(vinylidene fluoride) membrane anchored with silver nanoparticle with antibacterial activity, Synth. Met., 174 (2013) 1–5.

[18] E. Mahmoudi, L.Y. Ng, A.W. Mohammad, M.M. Ba-Abbad, Z. Razzaz, Enhancement of polysulfone membrane with integrated ZnO nanoparticles for the clarification of sweetwater, Int. J. Environ. Sci. Technol., 15 (2018) 561–570.

[19] S.R. Lakhotia, M. Mukhopadhyay, P. Kumari, Iron oxide (FeO) nanoparticles embedded thin-film nanocomposite nanofiltration (NF) membrane for water treatment, Sep. Purif. Technol., 211 (2019) 98–107.

[20] S. Ayyaru, Y.-H. Ahn, Fabrication and separation performance of polyethersulfone/sulfonated TiO_2 (PES–STiO$_2$) ultrafiltration membranes for fouling mitigation, J. Ind. Eng. Chem., 67 (2018) 199–209.

[21] S.H. Lee, B.H. Jun, Silver nanoparticles: synthesis and application for nanomedicine, Int. J. Mol. Sci., 20 (2019) 865, doi: 10.3390/ijms20040865.

[22] M. Sile-Yuksel, B. Tas, D.Y. Koseoglu-Imer, I. Koyuncu, Effect of silver nanoparticle (AgNP) location in nanocomposite membrane matrix fabricated with different polymer type on antibacterial mechanism, Desalination, 347 (2014) 120–130.

[23] Y. Chen, J. Dang, Y. Zhang, H. Zhang, J. Liu, Preparation and antibacterial property of PES/$AgNO_3$ three-bore hollow fiber ultrafiltration membranes, Water Sci. Technol., 67 (2013) 1519–1524.

[24] B.K. Chaturvedi, A.K. Ghosh, V. Ramachandhran, M.K. Trivedi, M.S. Hanra, B.M. Misra, Preparation, characterization and performance of polyethersulfone ultrafiltration membranes, Desalination, 133 (2001) 31–40.

[25] A.K. Hołda, I.F.J. Vankelecom, Understanding and guiding the phase inversion process for synthesis of solvent resistant nanofiltration membranes, J. Appl. Polym. Sci., 132 (2015) 42130, doi: 10.1002/app.42130.
[26] A. Abdel-Karim, T.A. Gad-Allah, A.S. El-Kalliny, S.I.A. Ahmed, E.R. Souaya, M.I. Badawy, M. Ulbricht, Fabrication of modified polyethersulfone membranes for wastewater treatment by submerged membrane bioreactor, Sep. Purif. Technol., 175 (2017) 36–46.
[27] K. Kotlhao, I.A. Lawal, R.M. Moutloali, M.J. Klink, Antifouling properties of silver-zinc oxide polyamide thin film composite membrane and rejection of 2-chlorophenol and 2,4-dichlorophenol, Membranes, 9 (2019) 96, doi: 10.3390/membranes9080096.
[28] J.-H. Li, X.-S. Shao, Q. Zhou, M.-Z. Li, Q.-Q. Zhang, The double effects of silver nanoparticles on the PVDF membrane: surface hydrophilicity and antifouling performance, Appl. Surf. Sci., 265 (2013) 663–670.
[29] L. Huang, S. Zhao, Z. Wang, J. Wu, J. Wang, S. Wang, In situ immobilization of silver nanoparticles for improving permeability, antifouling and anti-bacterial properties of ultrafiltration membrane, J. Membr. Sci., 499 (2016) 269–281.
[30] K.A.M. Said, R.L. Jamain, N.S.M. Sutan, N.A.M. Alipah, Enhanced permeation performance with incorporation of silver nitrate onto polymeric membrane, J. Mech. Eng. Sci., 12 (2018) 3811–3824.
[31] W.-R. Li, X.-B. Xie, Q.-S. Shi, H.-Y. Zeng, Y.-S. Ou-Yang, Y.-B. Chen, Antibacterial activity and mechanism of silver nanoparticles on *Escherichia coli*, Appl. Microbiol. Biotechnol., 85 (2010) 1115–1122.
[32] C. Ursino, R. Castro-Muñoz, E. Drioli, L. Gzara, M.H. Albeirutty, A. Figoli, Progress of nanocomposite membranes for water treatment, Membranes, 8 (2018) 18, doi: 10.3390/membranes8020018.
[33] X. Dong, H.D. Shannon, A. Amirsoleimani, G.M. Brion, I.C. Escobar, Thiol-affinity immobilization of casein-coated silver nanoparticles on polymeric membranes for biofouling control, Polymers, 11 (2019) 2057, doi: 10.3390/polym11122057.
[34] G. Xiao, X. Zhang, W. Zhang, S. Zhang, H. Su, T. Tan, Visible-light-mediated synergistic photocatalytic antimicrobial effects and mechanism of Ag-nanoparticles@chitosan–TiO_2 organic–inorganic composites for water disinfection, Appl. Catal., B, 170–171 (2015) 255–262.
[35] E.D. Cavassin, L.F.P. de Figueiredo, J.P. Otoch, M.M. Seckler, R.A. de Oliveira, F.F. Franco, V.S. Marangoni, V. Zucolotto, A.S.S. Levin, S.F. Costa, Comparison of methods to detect the in vitro activity of silver nanoparticles (AgNP) against multidrug resistant bacteria, J. Nanobiotechnol., 13 (2015) 64, doi: 10.1186/s12951-015-0120-6.

Supplementary information

S1. Viscosity measurements

Table S1
Viscosity and conductivity of PES and PES-AgNPs solutions

Membrane code	R^2	Viscosity (cP)	Conductivity (μS cm^{-1})
PES-0.0AgNPs	0.9999	270.75	1.5313 ± 0.0015
PES-0.5AgNPs	0.9998	283.22	3.2867 ± 0.0058
PES-1.0AgNPs	0.9998	319.55	4.3267 ± 0.0115
PES-2.0AgNPs	0.9998	349.08	5.3100 ± 0.0173

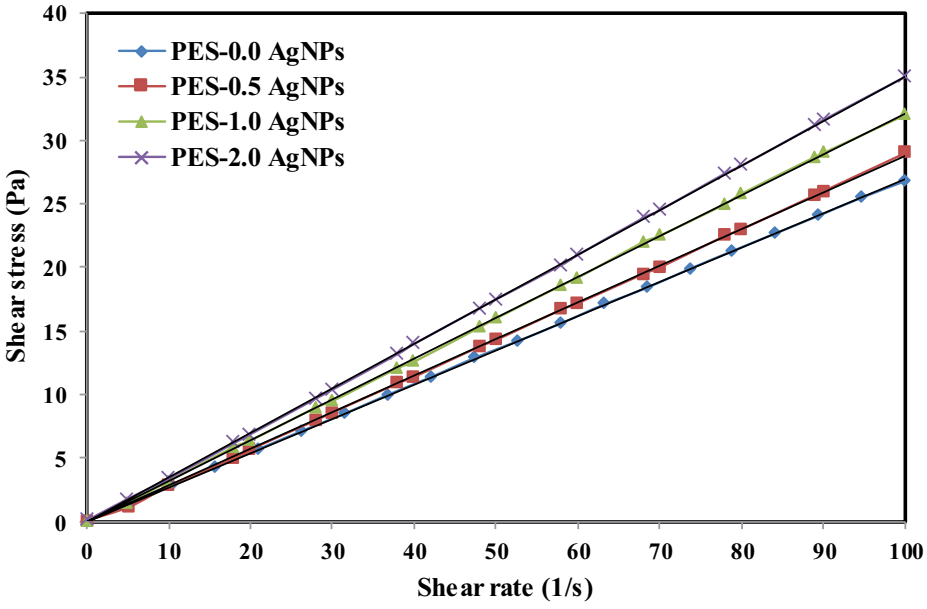

Fig. S1. Shear stress behavior with a shear rate of PES and PES-AgNPs solutions.

S2. Energy-dispersive X-ray spectroscopy

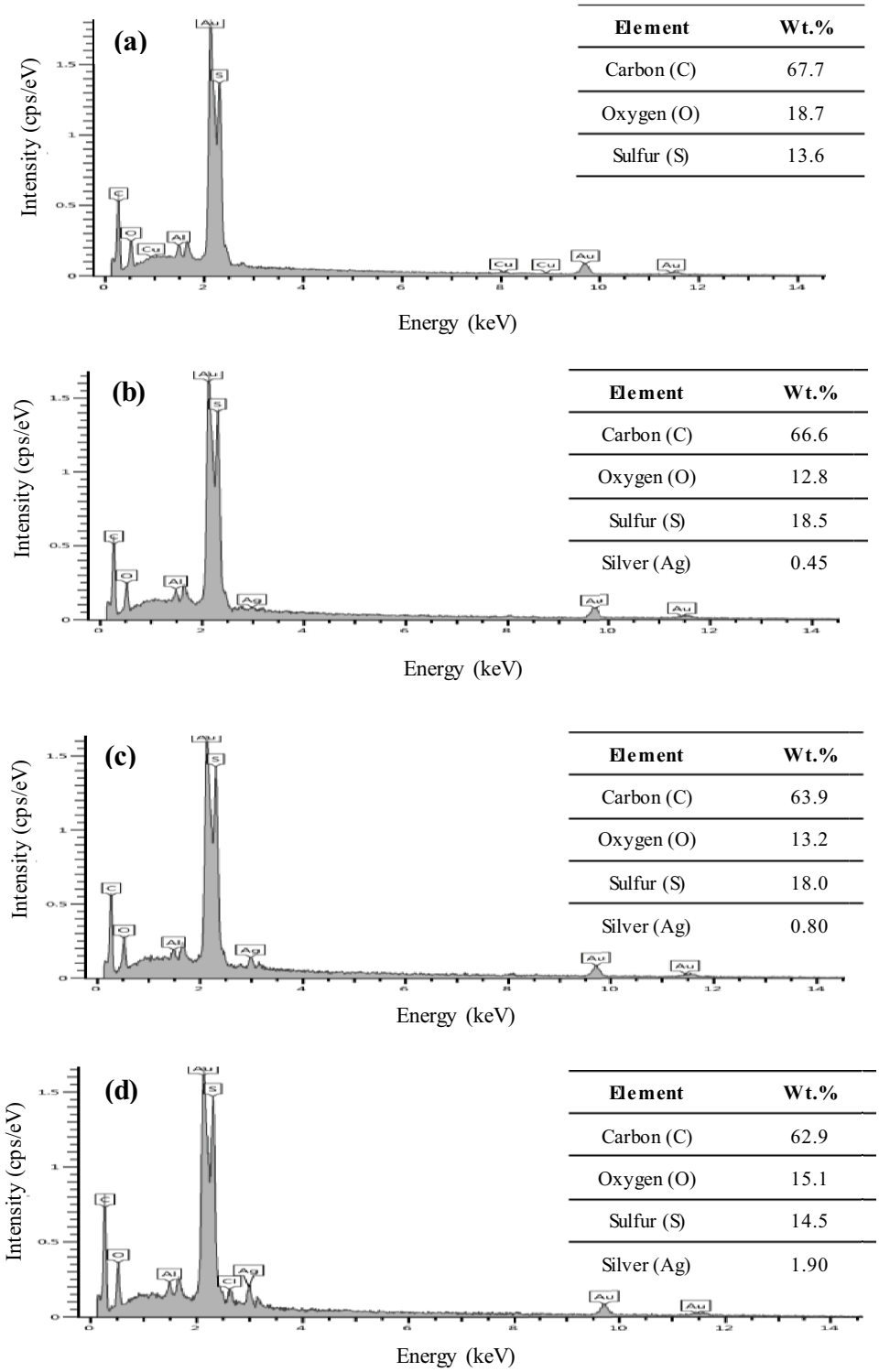

Element	Wt.%
Carbon (C)	67.7
Oxygen (O)	18.7
Sulfur (S)	13.6

Element	Wt.%
Carbon (C)	66.6
Oxygen (O)	12.8
Sulfur (S)	18.5
Silver (Ag)	0.45

Element	Wt.%
Carbon (C)	63.9
Oxygen (O)	13.2
Sulfur (S)	18.0
Silver (Ag)	0.80

Element	Wt.%
Carbon (C)	62.9
Oxygen (O)	15.1
Sulfur (S)	14.5
Silver (Ag)	1.90

Fig. S2. Energy-dispersive X-ray spectroscopy of (a) PES-0.0AgNPs, (b) PES-0.5AgNPs, (c) PES-1.0AgNPs and (d) PES-2.0AgNPs membranes.

S3. True stress-true strain curve

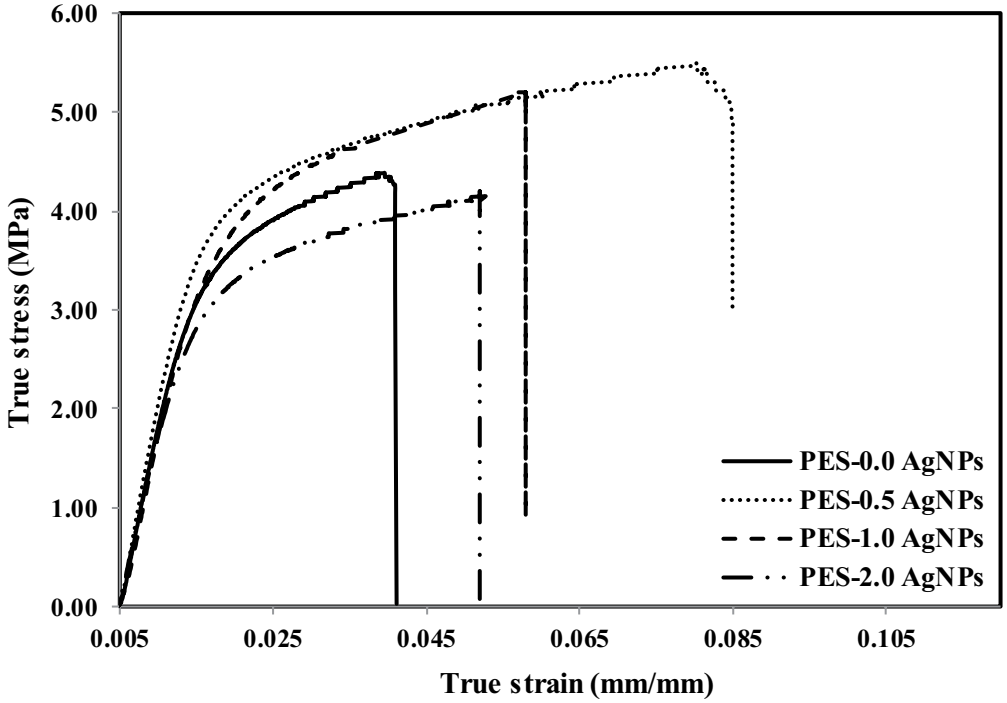

Fig. S3. True stress-true strain curve of PES casting membranes with and without AgNPs modification.

S4. Biofouling properties

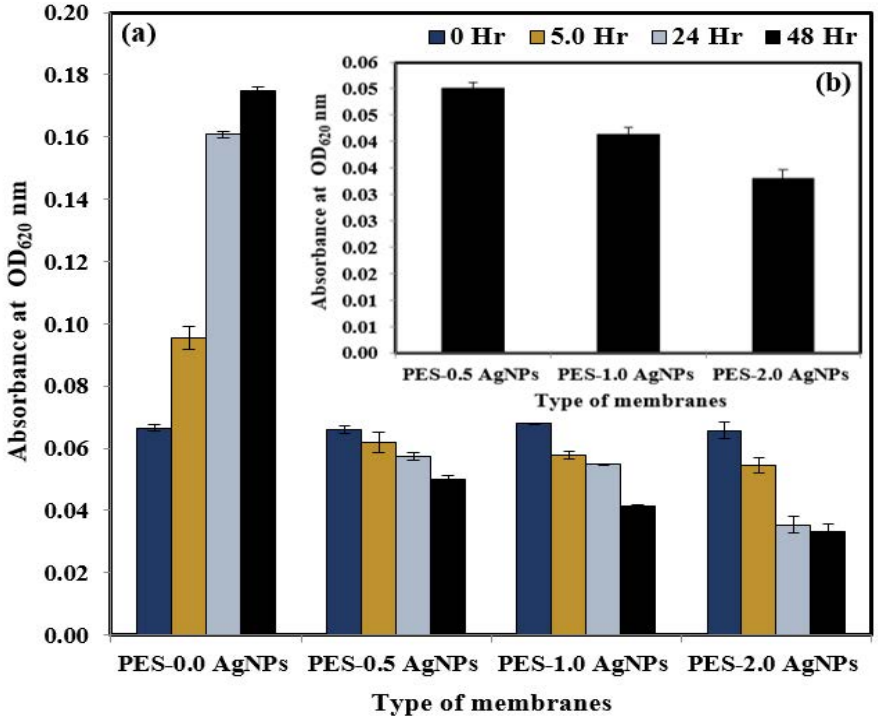

Fig. S4. (a) Effect of AgNPs embedded in PES membrane in different concentration in light condition (30–35 W m^{-2}) on *Bacillus subtilis* bacterium after two inhibition days and (b) effect of AgNPs concentration on antibacterial properties of PES-AgNPs nanocomposite membranes over 48 h of testing time.

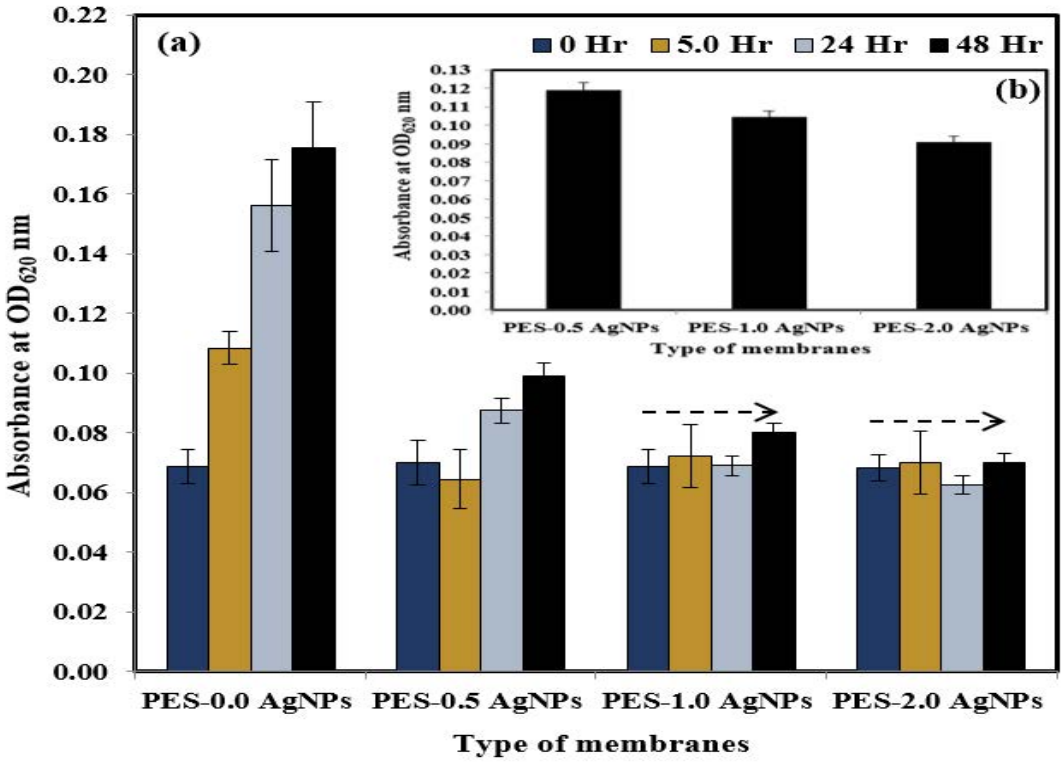

Fig. S5. (a) Effect of AgNPs embedded in PES membrane in different concentrations in dark condition (0 W m^{-2}) on *Bacillus subtilis* bacterium after two inhibition days and (b) effect of AgNPs concentration on antibacterial properties of PES-AgNPs nanocomposite membranes over 48 h of testing time.

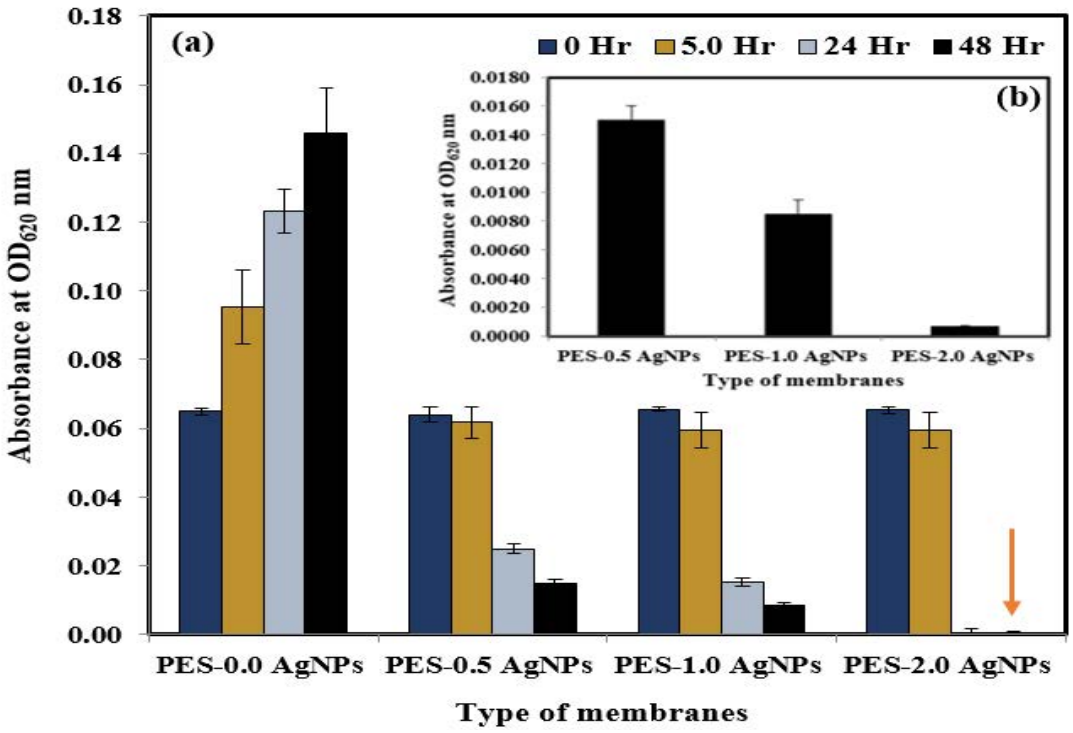

Fig. S6. (a) Effect of AgNPs embedded in PES membrane in different concentrations in light condition (30–35 W m^{-2}) on *Escherichia coli* bacterium after two inhibition days and (b) effect of AgNPs concentration on antibacterial properties of PES-AgNPs nanocomposite membranes over 48 h of testing time.

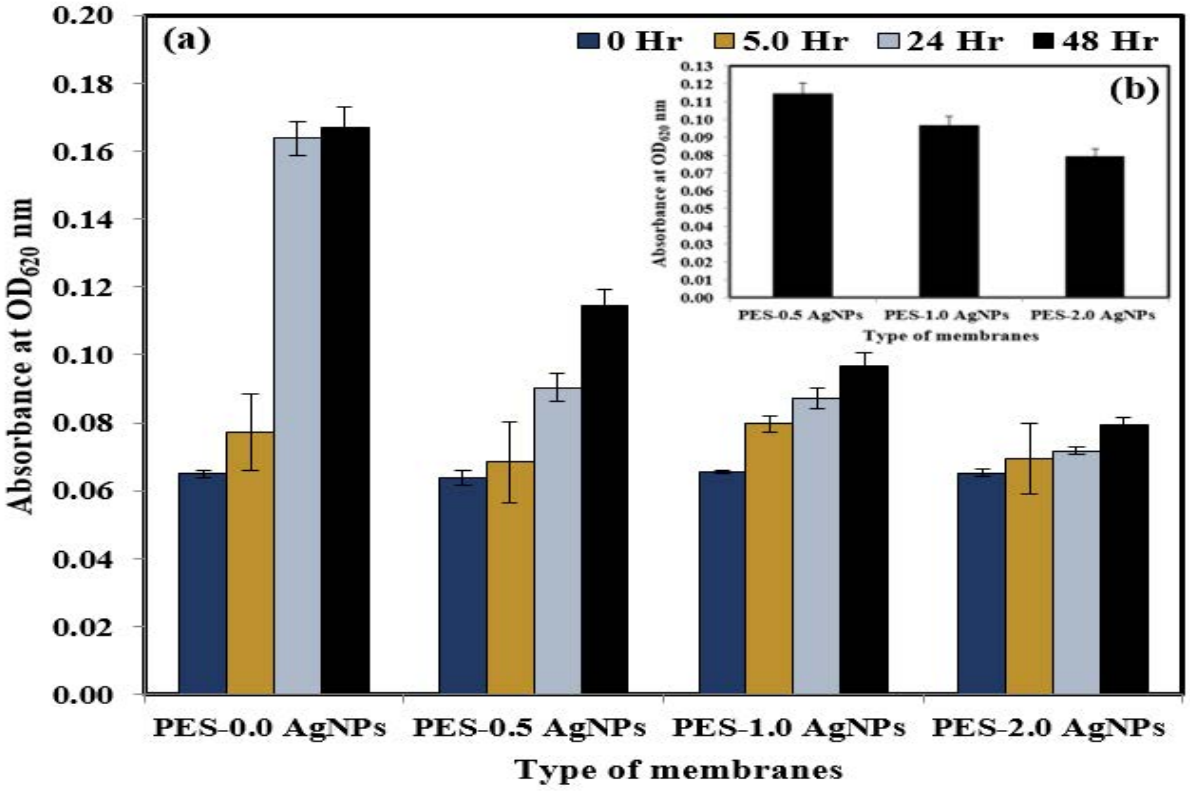

Fig. S7. (a) Effect of AgNPs embedded in PES membrane in different concentrations in dark condition (0 W m^{-2}) on *Escherichia coli* bacterium after two inhibition days and (b) effect of AgNPs concentration on antibacterial properties of PES-AgNPs nanocomposite membranes over 48 h of testing time.